

## Spreading Behavior of Molybdenum Trioxide on Alumina and Silica: A Raman Microscopy Study

JÜRGEN LEYRER, DANIELA MEY, AND HELMUT KNÖZINGER<sup>1</sup>

*Institut für Physikalische Chemie, Universität München, Sophienstrasse 11, 8000 München 2, West Germany*

Received November 13, 1989; revised March 2, 1990

The wetting of alumina by molybdenum trioxide has been demonstrated by Raman microscopy. Special specimens, which consisted of an alumina wafer in contact with a molybdenum trioxide wafer, were prepared for this purpose. Concentration profiles across the sharp dividing line between the two oxides were measured with a Raman microscope after thermal treatment at 800 K in a stream of dry O<sub>2</sub> or O<sub>2</sub> saturated with water vapor. The molybdenum oxide was transported over the alumina surface for several hundred micrometers. In contrast, in a similar wafer with silica no transport of molybdenum oxide could be observed. The results suggest that neither gas-phase transport nor surface diffusion in a concentration gradient provide major contributions to the spreading process. A solid–solid wetting process is considered to best describe the observed phenomena, the decrease in surface free energy being the dominant driving force for the spreading of molybdenum oxide over alumina. © 1990 Academic Press, Inc.

### INTRODUCTION

The great current interest in molybdena/alumina catalysts is due to the enormous technological importance of this class of catalyst precursors for hydrodesulfurization (HDS) and other hydrotreating reactions. Typically, these materials are prepared by impregnation (1, 2) of the alumina support from aqueous solutions containing an appropriate molybdenum compound (usually (NH<sub>4</sub>)<sub>6</sub> Mo<sub>7</sub>O<sub>24</sub>) followed by drying and calcination at temperatures around 770 K. The catalytic materials obtained in this way are frequently considered to develop a monolayer on the support consisting of molybdenum–oxygen polyhedra. The anchoring of three-dimensional Mo<sub>7</sub>O<sub>24</sub><sup>6–</sup> islands onto the alumina support surface appears to be a more likely structural model (see Refs. (1) and (3) and references therein). This surface polyanion must have an unknown number of protons attached to it for charge compensation, the number of protons depending on the number of Mo–O–Al anchoring

bonds to the surface. The heptamolybdate anion has been suggested to be the crucial precursor species for an active sulfided catalyst (1, 4).

In a series of papers, Xie and co-workers (5–9) concluded from X-ray photoelectron spectroscopy (XPS) and X-ray diffraction (XRD) studies that MoO<sub>3</sub> spontaneously spreads over the surface of alumina in physical mixtures of the two oxides when these are thermally treated at temperatures around 670–770 K in air. We have earlier reported (10–12) supporting evidence for this phenomenon as obtained by ion scattering spectroscopy (ISS). Raman spectroscopy provided additional information on the structure of the molybdenum–oxygen species present on the alumina surface after the spreading had occurred (2, 10–13). The vibrational spectra demonstrated the importance of the gas atmosphere during thermal treatment: only MoO<sub>3</sub> (which was X-ray amorphous) could be detected in absolutely dry O<sub>2</sub> atmosphere, while in the presence of water vapor the surface heptamolybdate was formed. The latter material had the same activity for thiophene HDS as the con-

<sup>1</sup> To whom all correspondence should be addressed.

ventionally impregnated catalyst having the same molybdenum loading, while the former material was significantly less active (1, 14).

Interestingly, spreading could not be observed in mixtures of  $\text{MoO}_3$  and  $\text{SiO}_2$  (12). The observations could be explained phenomenologically (2, 10–12, 15–18), but the microscopic mechanism of the spreading process is still unknown.

In the present paper we report on studies carried out by means of a Raman microscope; the aim of the work was to test whether detectable contributions from gas-phase transport would occur, and whether a possible surface transport would occur over macroscopic distances. To answer these questions, special samples were prepared in which wafers of  $\text{MoO}_3$  and  $\text{Al}_2\text{O}_3$  or  $\text{SiO}_2$  were brought into contact with a sharp dividing line. Concentration profiles across this dividing line were measured by Raman microscopy after thermal treatments of the wafers with a lateral resolution of ca. 25  $\mu\text{m}$ .

## EXPERIMENTAL

### 1. Materials

$\gamma\text{-Al}_2\text{O}_3$  was prepared by calcination of the hydroxide PURAL SB (Condea, Brunsbüttel, FRG) in air at 1048 K for 24 h. The resulting oxide had a  $\text{N}_2$  BET surface area of 123  $\text{m}^2\text{g}^{-1}$ . The  $\text{SiO}_2$  used was Aerosil 200 prepared by flame hydrolysis of the chloride and provided by Degussa (Hanau, FRG). It had a BET surface area of 200  $\text{m}^2\text{g}^{-1}$ .

$\text{MoO}_3$  was a Merck product (AR grade). It had a BET surface area of less than 5  $\text{m}^2\text{g}^{-1}$ .

$\text{O}_2$  and Ar were from Linde AG and had 99.998% nominal purity. The gases were further dried by passing them through a column containing freshly activated 4Å molecular sieve (Merck).

### 2. Sample Preparation

$\gamma\text{-Al}_2\text{O}_3$  or  $\text{SiO}_2$  were first pressed at 200  $\text{kp cm}^{-2}$  ( $1\text{kp} = 9.81\text{N}$ ) between two mica sheets for ca. 30 s to obtain a thin wafer. A sharp edge was prepared by cutting the wa-

fer with a scalpel.  $\text{MoO}_3$  powder (ground in an agate mortar for 5 min) was then placed on the mica sheet, homogeneously distributed, and brought into close contact with the sharp  $\gamma\text{-Al}_2\text{O}_3$  or  $\text{SiO}_2$  edge. Care was taken not to place any  $\text{MoO}_3$  powder onto the surface of the  $\gamma\text{-Al}_2\text{O}_3$  or  $\text{SiO}_2$  wafer. A short piece of Pt wire (0.5 mm in diameter) was also placed at the edge. This could later be used as the zero of the distance scale. This combination of wafer and  $\text{MoO}_3$  powder was then covered with a second mica sheet and pressed at 100  $\text{kp cm}^{-2}$  for ca. 30 s. Sufficiently stable wafers in which the two oxides were in contact across a well-defined dividing line were thus obtained.

These samples were placed in a glass reactor for thermal treatments at 770–800 K for up to 200 h. A dry argon flow (50  $\text{cm}^3\text{min}^{-1}$ ) was passed over the sample during the initial warm-up period. When the temperature of 800 K was reached, an oxygen flow (50  $\text{cm}^3\text{min}^{-1}$ ), either dry or saturated with water vapor at a partial pressure of 56 hPa, was admitted (to avoid reduction of  $\text{MoO}_3$ ). The saturation of the  $\text{O}_2$  flow with water vapor was performed with a temperature-controlled saturator, which was described earlier (19).

### 3. Raman Spectroscopy

Laser Raman spectra were recorded in the wavenumber range 800–1200  $\text{cm}^{-1}$  on a computer-controlled Dilor OMARS 90 spectrometer, the design of which was described by Deffontaine *et al.* (20). The spectrometer was equipped with an optical multichannel analyzer (OMA) Model IRY 512 from Spectroscopy Instruments. For Raman microscopy, an Olympus microscope Model BHT was connected to the spectrometer and in this way laterally resolved spectra of the specimen were obtained. The sample wafer was kept in ambient atmosphere in these studies.

The 514.5-nm line of a Spectra Physics  $\text{Ar}^+$  ion laser Model 2025-03 was used for excitation. The laser power at the sample was typically limited to 15 mW. The lateral

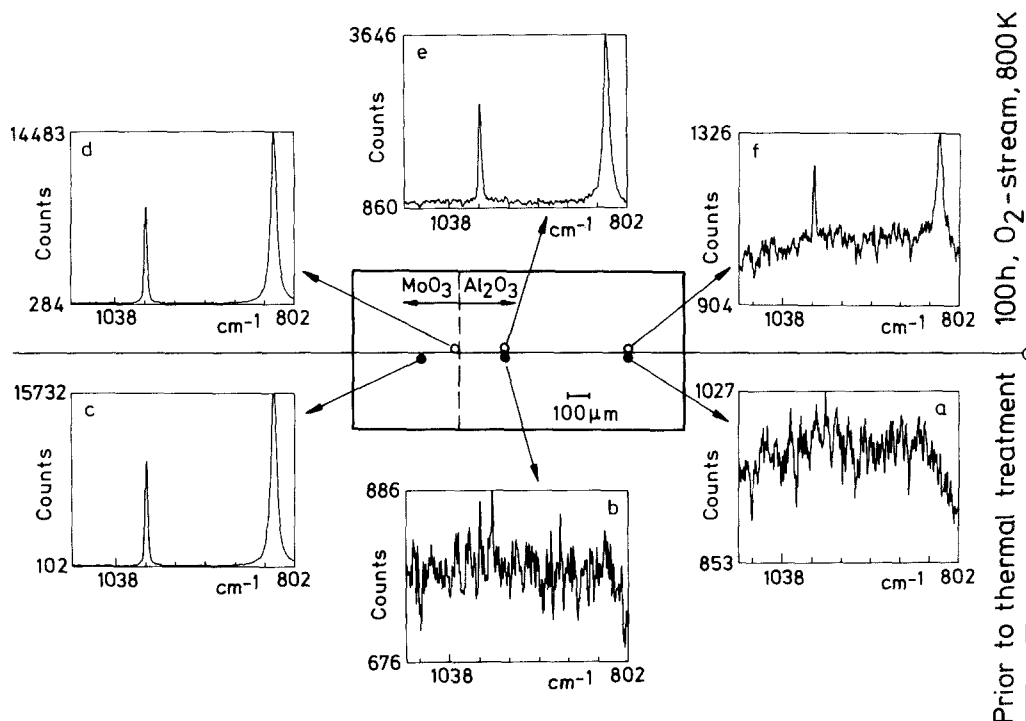


FIG. 1. Raman spectra of an untreated MoO<sub>3</sub>/Al<sub>2</sub>O<sub>3</sub> wafer (a–c) and after thermal treatment (d–f) at 800 K in a dry O<sub>2</sub> flow for 100 h at the indicated positions.

resolution was estimated to be ca. 25  $\mu\text{m}$ . The spectra were recorded with a spectral resolution of 2.5  $\text{cm}^{-1}$  and the wavenumber accuracy was  $\pm 2 \text{ cm}^{-1}$ .

## RESULTS

Laterally resolved Raman spectra were recorded across the dividing line of the specimens prior to and after thermal treatments. Typical spectra for MoO<sub>3</sub>/Al<sub>2</sub>O<sub>3</sub> prior to thermal treatment (spectra a–c) and after calcination at 800 K in dry flowing O<sub>2</sub> for 100 h (spectra d–f) are shown in Fig. 1. A schematic representation of the MoO<sub>3</sub>/Al<sub>2</sub>O<sub>3</sub> wafer is illustrated in the center of the figure which indicates the locations at which the spectra shown were taken. As expected, only noisy background without any characteristic features is recorded on the Al<sub>2</sub>O<sub>3</sub> part of the wafer prior to thermal treatment (spectra a and b), while the two strongest Raman bands of MoO<sub>3</sub> at 819 and 999  $\text{cm}^{-1}$

(22) are clearly detected on the MoO<sub>3</sub> half of the wafer (spectrum c). In contrast, after thermal treatment at 800 K in dry O<sub>2</sub> flow for 100 h these Raman bands are clearly detectable at distances of ca. 170  $\mu\text{m}$  (spectrum e) and even 660  $\mu\text{m}$  from the dividing line (spectrum f). This indicates that MoO<sub>3</sub> was transported during the thermal treatment over macroscopic distances across the dividing line and that the only detectable chemical species formed on the Al<sub>2</sub>O<sub>3</sub> surface is MoO<sub>3</sub>. The absolute intensities of the characteristic MoO<sub>3</sub> Raman lines and the signal-to-noise ratio clearly decrease with increasing distance from the dividing line in the direction of the Al<sub>2</sub>O<sub>3</sub> part of the wafer (see Fig. 1, spectra d–f), suggesting that a concentration profile has developed across the dividing line. A typical profile is shown in Fig. 2, where the relative peak intensity of the MoO<sub>3</sub> Raman line at 999  $\text{cm}^{-1}$  (referenced to the intensity of this line in the MoO<sub>3</sub>

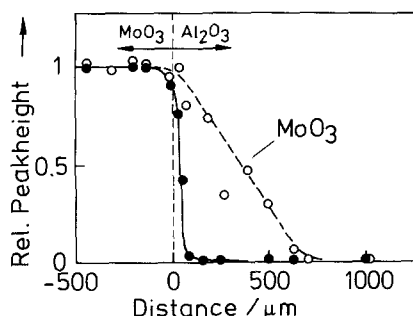


FIG. 2. Relative peak heights of the characteristic MoO<sub>3</sub> band at 999 cm<sup>-1</sup> of a MoO<sub>3</sub>/Al<sub>2</sub>O<sub>3</sub> wafer prior to (●) and after (○) thermal treatment for 100 h at 800 K in dry O<sub>2</sub> flow plotted vs the distance from the dividing line between MoO<sub>3</sub> and Al<sub>2</sub>O<sub>3</sub>.

part of the wafer) is plotted against the distance from the dividing line for samples prior to and after thermal treatment. Comparison of the two profiles in this figure clearly demonstrates the transport of MoO<sub>3</sub> over several hundred micrometers under the experimental conditions applied. It is important to note that almost identical profiles were obtained irrespective of the direction of the O<sub>2</sub> flow.

Analogous experiments were carried out applying an O<sub>2</sub> flow which was saturated with 56 hPa H<sub>2</sub>O vapor. Typical spectra obtained at various positions of the wafer prior to and after thermal treatment are shown in Fig. 3. The spectra for the untreated sample wafer match those shown in Fig. 1, indicating that the MoO<sub>3</sub> concentration steeply decays across the dividing line (see Fig. 4). After thermal treatment a new broad spectral feature with a maximum at 965 cm<sup>-1</sup> develops on the Al<sub>2</sub>O<sub>3</sub> part of the wafer up to distances of ca. 1000 μm from the dividing line. This band corresponds to the Mo=O stretching mode of a surface polymolybdate (probably Mo<sub>7</sub>O<sub>24</sub><sup>6-</sup>) as reported earlier (12, 22–24). Hence, in agreement with our previous results obtained on mixtures of oxide powders (10–13), not only spreading but also chemical transformation of the MoO<sub>3</sub> into a surface polymolybdate occurs in the presence of water vapor. As indicated by

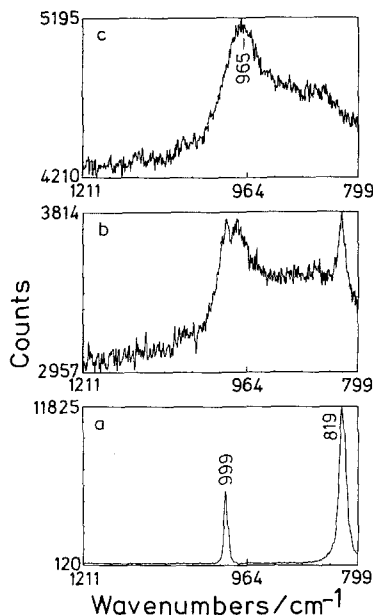


FIG. 3. Raman spectra of a MoO<sub>3</sub>/Al<sub>2</sub>O<sub>3</sub> wafer after thermal treatment for 100 h at 800 K in a water vapor-saturated O<sub>2</sub> flow taken at (a) the dividing line, (b) 200 μm from the dividing line, and (c) 900 μm from the dividing line.

the dependence of the relative intensities on distance from the dividing line (concentration profiles) as shown in Fig. 4, the polymolybdate formation occurs only on the Al<sub>2</sub>O<sub>3</sub> surface, while the MoO<sub>3</sub> profiles are identi-

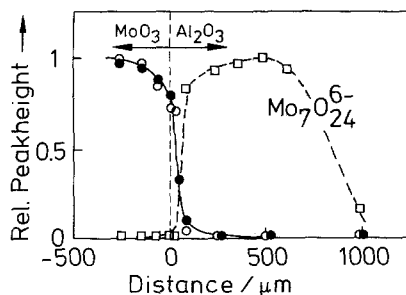


FIG. 4. Relative peak heights of the characteristic Raman bands of MoO<sub>3</sub> at 999 cm<sup>-1</sup> and of the surface polymolybdate at 965 cm<sup>-1</sup> prior to (●) and after (○ and □) thermal treatment for 100 h at 800 K in water vapor-saturated O<sub>2</sub> flow plotted vs the distance from the dividing line between MoO<sub>3</sub> and Al<sub>2</sub>O<sub>3</sub>.

cal before and after thermal treatment. The relative intensities of the polymolybdate bands at 965 cm<sup>-1</sup> as plotted in Fig. 4 were referenced to the maximum intensity of this band measured at ca. 500 μm from the dividing line.

Entirely different results were obtained with the MoO<sub>3</sub>/SiO<sub>2</sub> wafer. Even after thermal treatment for 200 h under otherwise identical conditions in either dry or water vapor-saturated O<sub>2</sub> flow, neither MoO<sub>3</sub> nor polymolybdate species could be detected on the SiO<sub>2</sub> part of the wafer. As an example of this behavior, the concentration profiles after calcination at 770 K in dry O<sub>2</sub> flow for 100 and 200 h are compared in Fig. 5 with that of the wafer prior to thermal treatment. Within the limits of the lateral resolution of the technique, all three profiles are identical. This undoubtedly suggests that transport of MoO<sub>3</sub> across the dividing line between the two oxides has not occurred in this case under the applied experimental conditions. Even in the presence of water during thermal treatment the concentration profile for MoO<sub>3</sub> was identical to those shown in Fig. 5 and no indication for a surface molybdate could be detected. These observations are in complete agreement with earlier results obtained for physical mixtures of MoO<sub>3</sub> and SiO<sub>2</sub>. ISS had shown that spreading did not occur in this system and the only detectable

species in the Raman spectra even in the presence of water vapor during thermal treatment was MoO<sub>3</sub> (12).

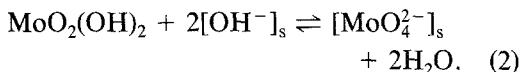
#### DISCUSSION

The present studies clearly demonstrate that spreading of MoO<sub>3</sub> occurred on the Al<sub>2</sub>O<sub>3</sub> surface in the presence and absence of water vapor, while this was not the case with the SiO<sub>2</sub> surface. In addition, MoO<sub>3</sub> was converted into a surface polymolybdate on the Al<sub>2</sub>O<sub>3</sub> surface when water was present. These results are in complete agreement with previous results obtained for physical mixtures of the oxide combinations by means of ISS and Raman spectroscopy (10–13).

The chemical transformation of MoO<sub>3</sub> on the Al<sub>2</sub>O<sub>3</sub> surface was described (10–13) as being due to the intermediate formation of MoO<sub>2</sub>(OH)<sub>2</sub>, a reaction which does occur with low but nonnegligible yields under the experimental conditions (25, 26):



This oxyhydroxide is then assumed to react with hydroxyl groups [OH<sup>-</sup>]<sub>s</sub> to form a surface molybdate [MoO<sub>4</sub><sup>2-</sup>]<sub>s</sub>:



The [MoO<sub>4</sub><sup>2-</sup>]<sub>s</sub> species have been detected as intermediates (13). They undergo condensation with formation of the surface polymolybdate provided their local concentration becomes sufficiently high.

The spreading phenomenon itself was interpreted phenomenologically as a solid–solid wetting process (10–12, 15–18). The change in the surface free energy ΔF<sub>s</sub> was considered to be the driving force for the spreading process,

$$\Delta F_s = \gamma_{M,g} \Delta A_M - \gamma_{S,g} \Delta A_S + \gamma_{MS} \Delta A_{MS}, \quad (3)$$

where γ<sub>M,g</sub> and γ<sub>S,g</sub> are the areal surface free energies of MoO<sub>3</sub> and the support oxide, respectively, in contact with the gas phase and γ<sub>MS</sub> is the specific free interface energy.

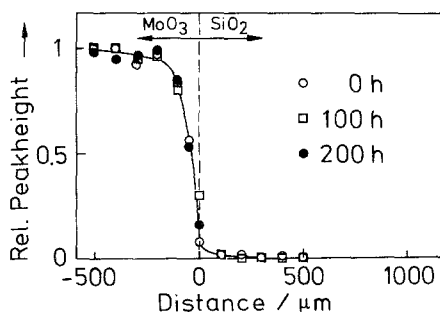


FIG. 5. Relative peak height of the characteristic Raman band of MoO<sub>3</sub> at 999 cm<sup>-1</sup> of a MoO<sub>3</sub>/SiO<sub>2</sub> wafer prior to (○) and after thermal treatment for 100 h (□) and 200 h (●) at 770 K in dry O<sub>2</sub> flow plotted vs the distance from the dividing line between MoO<sub>3</sub> and SiO<sub>2</sub>.

The  $\Delta A_M$ ,  $\Delta A_S$ , and  $\Delta A_{MS}$  are the corresponding changes in surface and interface areas. Spreading will occur if  $\Delta F_s < 0$ . Assuming  $|\Delta A_M| = |\Delta A_S| = |\Delta A_{MS}|$ , this requires

$$(\gamma_{M,g} + \gamma_{MS}) < \gamma_{S,g}. \quad (4)$$

Approximate surface free energies are known (27), and  $\gamma_{M,g}$  turns out to be smaller by about an order of magnitude than  $\gamma_{S,g}$  of both  $Al_2O_3$  and  $SiO_2$ . The interface free energies are unknown. It has been argued (12), however, that "chemical" interactions are likely to occur between  $MoO_3$  and  $Al_2O_3$  ( $Al_2(MoO_4)_3$  is formed in a solid state reaction at higher temperatures) while such interactions are not to be expected between  $MoO_3$  and  $SiO_2$  (no solid state reaction reported in the literature). Hence,  $\gamma_{MS}$  in Eq. (4) is favorable for spreading in the case of  $Al_2O_3$  and presumably unfavorable in the case of  $SiO_2$ . The different behaviors of the  $MoO_3/Al_2O_3$  and  $MoO_3/SiO_2$  could thus be explained on a thermodynamic basis.

The microscopic mechanism of the spreading process in those cases where it is thermodynamically possible, is, however, still unknown. Also, the present study cannot establish such transport mechanisms at a molecular level. However, certain processes can be excluded based on the present results.

$MoO_3$  is known to sublime slowly at temperatures around 800 K, the temperature applied during the thermal treatments as described above. Therefore, gas-phase transport might contribute to the transport of  $MoO_3$  onto the support surface. The experimental results, however, permit us to exclude measurable contributions of gas-phase transport. First, if gas-phase transport had occurred, S-shaped concentration profiles as shown in Fig. 2 would hardly have been built up, but rather the entire alumina part of the wafer would have been covered by  $MoO_3$ . Moreover, deposition of  $MoO_3$  would also have been expected on the  $SiO_2$  wafer, which was not observed. Second, if gas-phase transport were impor-

tant, the deposition of  $MoO_3$  on the  $Al_2O_3$  part of the wafer would have been dependent on the direction of the  $O_2$  flow, which was not the case.

The oxyhydroxide  $MoO_2(OH)_2$  has a higher vapor pressure than  $MoO_3$  (25, 26). This fact has been used to load  $MoO_3$  onto support oxides in packed columns by Sonnemans and Mars (28). We had therefore originally assumed (13) that the  $MoO_2(OH)_2$  species was the mobile species. This assumption, however, cannot explain the  $MoO_3$  mobility in the absence of water vapor. Gas-phase transport mediated by the oxyhydroxide can be excluded by the same arguments given in the previous paragraph. It must therefore be concluded that gas-phase transport is negligible and that surface transport must be responsible for the observed spreading phenomenon.

The Raman microscopy studies reported here indicate that the spreading of  $MoO_3$  is not a local phenomenon occurring exclusively at or very close (on an atomic scale) to a contact zone between a  $MoO_3$  particle and an  $Al_2O_3$  particle, but transport rather occurs over macroscopic distances (several 100  $\mu m$  under the applied experimental conditions). This observation is in good agreement with the elegant high-resolution TEM results of Hayden *et al.* (29).

The melting point  $T_m$  of  $MoO_3$  is 1068 K, and hence, the Tammann temperature  $T_T \cong 0.5 T_m$  is calculated to be 534 K. Therefore, mobility of  $MoO_3$  at the temperatures of the present experiments is undoubtedly expected and one might describe the surface transport in terms of diffusion in a concentration gradient across the dividing line between the two oxides. This mechanism, however, must also be rejected, since in this case the driving forces would be the same for the  $MoO_3/Al_2O_3$  and  $MoO_3/SiO_2$  combinations and a broadening of the concentration profile across the dividing line would be expected in both cases. This, however, was not observed (compare Figs. 2 and 5). Haber (17) also concluded that surface diffusion should be slow in the temperature range

concerned due to the relatively high values of the lattice energy of oxides.

It must therefore be concluded that a significant decrease in surface free energy  $\Delta F_s$  in the case of MoO<sub>3</sub>/Al<sub>2</sub>O<sub>3</sub> acts as the dominant driving force for the spreading, which can thus be described as wetting of one solid by a second solid. Close inspection of the concentration profiles of Figs. 2 and 4 shows that in the presence of water vapor under otherwise identical conditions the molybdenum species are transported over a somewhat larger distance than those in the absence of water vapor. Although the reason for this observation is not entirely clear, it is probably due to a modification of the surface free energies by adsorption of water.

#### CONCLUSIONS

The results of the present Raman microscopy study permit the following conclusions to be drawn:

1. MoO<sub>3</sub> spreads on the surface of alumina. The transport can occur over macroscopic distances, i.e., several hundred micrometers in the present case.

2. In contrast, spreading does not occur on silica surfaces.

3. Gas-phase transport can be excluded as the dominant mechanism, at least at the temperatures applied in the experiments described. This applies also when thermal treatments are carried out in the presence of water vapor, under which conditions MoO<sub>2</sub>(OH)<sub>2</sub> is formed and acts as an intermediate in surface polymolybdate formation.

4. Surface diffusion in a concentration gradient can also be rejected as a major mechanism of spreading.

5. The experimental results can best be explained by a solid–solid wetting process, in which the decrease in surface free energy is to be considered as the dominant driving force for spreading. The different behavior of Al<sub>2</sub>O<sub>3</sub> and SiO<sub>2</sub> can be understood on these grounds by assuming “chemical” interactions between MoO<sub>3</sub> and Al<sub>2</sub>O<sub>3</sub> which

lead to a favorable interface energy, which is not the case for MoO<sub>3</sub> and SiO<sub>2</sub>. These considerations are in full agreement with experimental results obtained for physical mixtures of powders of the various oxide combinations (10–12).

6. Wetting processes of this kind have been reported to be important steps in the mechanisms of solid state reactions (30, 31).

7. It is suggested that solid–solid wetting may play an important role in catalyst preparation and regeneration, particularly for supported oxides.

#### ACKNOWLEDGMENTS

This work was financially supported by the Deutsche Forschungsgemeinschaft, the Fonds der Chemischen Industrie, and the Bundesministerium für Forschung und Technologie.

#### REFERENCES

1. Knözinger, H., in “Proceedings, 9th International Congress on Catalysis, Calgary, 1988” (M. J. Phillips and M. Ternan, Eds.), Vol. 5, p. 20. Chem. Institute of Canada, Ottawa, 1988.
2. Knözinger, H., *Mater. Science Forum* **25/26**, 223 (1988).
3. Butz, T., Vogdt, C., Lerf, A., and Knözinger, H., *J. Catal.* **116**, 31 (1989).
4. Chiplunker, P., Martinez, N. P., and Mitchell, P. C. H., *Bull. Soc. Chim. Belg.* **90**, 1319 (1981).
5. Liu, Y., Xie, Y., Ming, J., Liu, J., and Tang, Y., *J. Catal. (China)* **3**, 262 (1982).
6. Liu, Y., Xie, Y., Li, C., Zou, Z., and Tang, Y., *J. Catal. (China)* **5**, 234 (1984).
7. Xie, Y., Gui, L., Liu, Y., Zhao, B., Yang, N., Zhang, Y., Guo, Q., Duan, L., Huang, H., Cai, X., and Tang, Y., in “Proceedings, 8th International Congress on Catalysis Berlin, 1984,” Vol. 5, p. 147. Dechema, Frankfurt-am-Main, and Verlag Chemie, Weinheim, 1984.
8. Xie, Y., Gui, L., Liu, Y., Zhang, Y., Zha, B., Yang, N., Guo, Q., Duan, L., Huang, H., Cai, X., and Tang, Y., in “Adsorption and Catalysis on Oxide Surfaces” (M. Che and G. C. Bond, Eds.), p. 139. Elsevier, Amsterdam, 1985.
9. Liu, Y., Xie, Y., Xie, G., and Tang, Y., *J. Catal. (China)* **6**, 101 (1985).
10. Margraf, R., Leyrer, J., Knözinger, H., and Taglauer, E., *Surf. Sci.* **189/190**, 842 (1987).
11. Margraf, R., Leyrer, J., Taglauer, E., and Knözinger, H., *React. Kinet. Catal. Lett.* **35**, 261 (1987).
12. Leyrer, J., Margraf, R., Taglauer, E., and Knözinger, H., *Surf. Sci.* **201**, 603 (1988).
13. Leyrer, J., Zaki, M. I., and Knözinger, H., *J. Phys. Chem.* **90**, 4775 (1986).

14. Koranyi, T. I., Paál, Z., Leyrer, J., and Knözinger, H., in preparation.
15. Haber, J., in "Surface Properties and Catalysis by Non-Metals" (J. P. Bonnelle *et al.*, Eds.), p. 1. Reidel, Dordrecht, 1983.
16. Haber, J., in "Proceedings, 8th International Congress on Catalysis, Berlin, 1984," Vol. 1, p. 85. Dechema, Frankfurt-am-Main, and Verlag Chemie, Weinheim, 1984.
17. Haber, J., *Pure Appl. Chem.* **56**, 1663 (1984).
18. Haber, J., Machej, T., and Czeppe, T., *Surf. Sci.* **151**, 301 (1985).
19. Knözinger, H., and Ress, E., *Z. Phys. Chem.* **54**, 136 (1967).
20. Deffontaine, A., Bridoux, M., Delhay, M., Da Silva, E., and Hug, W., *Rev. Phys. Appl.* **19**, 415 (1984).
21. Beattie, I. R., and Gilson, T. R., *Proc. R. Soc. London A* **307**, 407 (1968).
22. Jeziorowski, H., and Knözinger, H., *J. Phys. Chem.* **83**, 1166 (1979).
23. Knözinger, H., and Jeziorowski, H., *J. Phys. Chem.* **82**, 2002 (1978).
24. Payen, E., Kasztelan, S., Grimblot, J., and Bonnelle, J. P., *J. Raman Spectrosc.* **17**, 233 (1986).
25. Glemser, O., and Wendland, H. G., *Angew. Chem.* **75**, 949 (1963).
26. Glemser, O., and Wendland, H. G., *Adv. Inorg. Radiochem.* **5**, 215 (1963).
27. Overbury, S. H., Bertránd, P. A., and Somorjai, G. A., *Chem. Rev.* **75**, 547 (1975).
28. Sonnemans, J., and Mars, P., *J. Catal.* **31**, 209 (1973).
29. Hayden, T. F., Dumesic, J. A., Sherwood, R. D., and Baker, R. T. K., *J. Catal.* **105**, 299 (1987).
30. Haber, J., and Ziołkowski, J., in "Proceedings, 7th Intern. Symp. Reactivity of Solids, Bristol, 1972" (J. S. Anderson, M. W. Roberts, and F. S. Stone, Eds.), p. 782. Chapman & Hall, London, 1972.
31. Ziołkowski, J., Kozłowski, R., Mocała, K., and Haber, J., *J. Solid State Chem.* **35**, 297 (1980).